Electron-impact vibrational excitation of polyatomic gases: Exploratory calculations

M. Cascella
Department of Chemistry, The University of Rome, Cittá Universitaria, 00185 Rome, Italy

R. Curik
J. Heyrovsky Institute of Physical Chemistry, Academy of Science of the Czech Republic, 18223 Prague 8, Czech Republic

F. A. Gianturco[a)]
Department of Chemistry, The University of Rome, Cittá Universitaria, 00185 Rome, Italy

N. Sanna
Supercomputing Center for University and Research, CASPUR, Cittá Universitaria, 00185 Rome, Italy

(Received 20 April 2000; accepted 7 November 2000)

We present model calculations for the inelastic cross sections of electron collisions with tetrahedral molecules XH_4 (X=C, Si, Ge) when only the molecular ''breathing'' mode, ν_1, is being excited. The collision energy range is well above the excited thresholds and up to 12 eV, where the adiabatic approximation for the inelastic T matrix is expected to hold. The results show the efficiency of the t_2 shape resonance in enhancing the inelastic process and the appearance, in the two heavier targets, of a further a_1 resonance in the inelastic channels of both molecules. The corresponding excitation rates are also computed together with estimates of the vibrational excitation functions. © *2001 American Institute of Physics.* [DOI: 10.1063/1.1336567]

I. INTRODUCTION

Recent years have witnessed a marked increase of interest in understanding fairly complicated, multicomponent molecular mixtures evolving under strongly nonequilibrium conditions, which are in turn created by the action of electrical fields, laser fields, and shock waves.[1,2] In all the above-mentioned cases the often numerous molecular species which are composing the gaseous mixture become energetically excited up to several levels of their vibrational ladder, be it within their ground electronic states or in one of their electronically excited states.[3] The necessary efforts have been fueled by the clear technological interest in such studies, which have been directed to the development of specific particle beams, of selected molecular lasers, and to designing low-temperature multicomponent molecular plasmas for chemical vapor deposition technology.[4]

Electron collisions within the molecular mixtures are often responsible for creating such nonequilibrium environments and yet knowledge of the distributions of the excitation/deexcitation probabilities (the particle inelastic cross sections) for even the simpler polyatomic gases like CO_2, H_2O, CH_4, etc., is still very scant despite the important role which such species have in making up the relevant mixtures that often initiate the technological process.

The reasons for this marked lack of data of technological interest are both experimental and theoretical, in the sense that the direct measurement of state-to-state excitation cross sections from electron–molecule scattering processes is fairly hard to carry out in the low-energy regimes which are of more direct interest[5] and, at the same time, the computational development of *ab initio* methods for treating the excitation of vibrational and electronic excitations of nonlinear, polyatomic targets is still in its infancy.[6]

In the present study we are interested in the development of nonempirical models that describe the electron–molecule interactions and the coupling between the kinetic energy of the impinging electron and one of the target vibrational modes. This exploratory study will deal with the simplest of them, i.e., the totally symmetric breathing mode of tetrahedral molecules. We intend to show that, under the physical conditions where the modeling is applicable, the present approach provides a strong reduction of the computational time while yielding rather reasonable values for the state-to-state cross sections and/or the rates.

The work is organized as follows. Section II briefly describes the interaction forces and the scattering equations we are using for treating the quantum electron–molecule dynamics. In Sec. III we add the coupling with the nuclear motion and describe the adiabatic simplification that we shall use here. Section IV describes our exploratory computations for the cross sections of the three molecules we are examining, i.e., CH_4, SiH_4, and GeH_4. Finally, Sec. V will present our conclusions.

II. THE SCATTERING EQUATIONS

A. Single center expansions

Resonant and nonresonant low-energy scattering of electrons from polyatomic targets can be studied theoretically (and computationally) at various levels of sophistication for the description of: (i) the electronuclear structure of the tar-

a)Electronic mail: fagiant@caspur.it

get molecule, (ii) the interaction forces between the bound particles and the impinging electron, and (iii) the dynamical formulation of the quantum scattering equations.[7]

Within an *ab initio*, parameter-free approach one could start with the target nuclei being kept fixed at their equilibrium geometry and their motion during the scattering process could then be decoupled from the other variables. This simplifying scheme goes under the name of the fixed nuclei approximation[8] and it strongly reduces the dimensionality of the coupled scattering equations for the dynamics. Furthermore, the target N electrons bound in a specific molecular electronic state (which, for the present purpose, is taken as unchanged during the scattering) can be described within a near-Hartree–Fock, self-consistent field (SCF) approximation by using the single-determinant (SD) description of the N occupied molecular orbitals (MOs). In our implementation of the scattering equations the occupied MOs of the targets are again expanded on a set of symmetry-adapted angular functions with their corresponding radial coefficients represented on a numerical grid.[9–11] In this approach, any arbitrary three-dimensional function describing a given electron, either one of the N bound electrons or the scattering electron, is expanded around a single center (SCE) usually taken to be the center of mass of the global $(N+1)$ electron molecular structure

$$F^{p\mu}(r,\hat{\mathbf{r}}|\mathbf{R})=\sum_{l,h} r^{-1} f_{lh}^{p\mu}(r|\mathbf{R}) X_{lh}^{p\mu}(\hat{\mathbf{r}}). \tag{1}$$

The above SCE representation refers to the μth element of the pth irreducible representation (IR) of the point group of the molecule at the nuclear geometry $\mathbf{R}$. The angular functions $X_{lh}^{p\mu}(\hat{\mathbf{r}})$ are symmetry adapted angular functions given by proper combination of spherical harmonics $Y_{lm}(\hat{\mathbf{r}})$,

$$X_{lh}^{p\mu}(\hat{\mathbf{r}})=\sum_{m} b_{lmh}^{p\mu} Y_{lm}(\hat{\mathbf{r}}). \tag{2}$$

The quantum scattering equations then evaluate the unknown radial coefficients of Eq. (1) for the $(N+1)$th continuum electron scattered off the molecular target

$$\left[\frac{d^2}{dr^2}-\frac{l(l+1)}{r^2}+2(E-\epsilon_\alpha)\right] f_{lh}^{p\mu\alpha}(r|\mathbf{R}) = 2\sum_{l'h'\beta'} \int dr' V_{lh,l'h'}^{p\mu,\alpha\beta}(r,r'|\vec{R}) f_{l'h'}^{p\mu,\beta}(r'|\mathbf{R}), \tag{3}$$

where E is the collision energy $E=k^2/2$ and ϵ_α is the electronic eigenvalue for the αth asymptotic state. The $p\mu$ indices now label the specific μth component of the pth IR that belongs to the αth electronic target state (initial state) coupled with the infinity of excited state IRs labeled collectively by β. The coupled partial integrodifferential equations (3) contain the kernel of the integral operator V, which is thus a sum of diagonal and nondiagonal terms that in principle can fully describe the electron–molecule interaction during the collision. The zeroth-order treatment yields the exact-static-exchange (ESE) representation of the electron–molecule interaction for the chosen target state (usually the ground state) at a given nuclear geometry $\mathbf{R}$. Introducing the assumption of having only a local e^-–molecule interaction one can further simplify Eq. (3) by writing

$$\left[\frac{d^2}{dr^2}-\frac{l_i(l_i+1)}{r^2}+k^2\right] f_{ij}^{p\mu}(r|\mathbf{R}) = \sum_{n} V_{in}^{p\mu}(r|\mathbf{R}) f_{nj}^{p\mu}(r|\mathbf{R}), \tag{4}$$

where the indices i, j, or n represent the ''angular channel'' $|lh\rangle$ and the potential coupling elements are given as

$$V_{in}^{p\mu}(r|\mathbf{R})=\langle X_i^{p\mu}(\hat{\mathbf{r}})|V(\mathbf{r}|\mathbf{R})|X_n^{p\mu}(\hat{\mathbf{r}})\rangle = \int d\hat{\mathbf{r}}\, X_i^{p\mu}(\hat{\mathbf{r}}) V(\mathbf{r}|\mathbf{R}) X_n^{p\mu}(\hat{\mathbf{r}}). \tag{5}$$

The numerical solutions of the coupled equation (4) will produce the relevant K-matrix elements, which will in turn yield the necessary expression for the elastic (rotationally summed) differential cross sections, obtained for scattering by randomly oriented molecules by averaging the scattering amplitude $f(\hat{k}\cdot\hat{r}|\alpha,\beta,\gamma)$ over all the angular values.[7]

B. Interaction forces

For a target which has a closed-shell electronic structure, as in the present examples, with n_{occ} doubly occupied orbitals φ_i, the potential can be written, for the case of electron scattering, as first given by its exact static+exchange contributions

$$V_{\mathrm{ESE}}(\mathbf{r})=\sum_{\gamma=1}^{M}\frac{Z_\gamma}{|\mathbf{r}-\mathbf{R}_\gamma|}+\sum_{i=1}^{n_{\mathrm{occ}}}(2\hat{J}_i-\hat{K}_i), \tag{6}$$

where $\hat{J}_i$ and $\hat{K}_i$ are the usual local static potential and the nonlocal exchange potential operators, respectively. The index γ labels one of the M nuclei located at the coordinate $\mathbf{R}_\gamma$ in the center-of-mass, molecular (body) frame of reference (BF). Electron–molecule scattering cross sections (integral and differential) which are computed using the V_{ESE} potential of above usually only give some agreement with experimental data of elastic scattering at energies away from resonant features but turn out to be not at all realistic when used for resonant scattering.[7]

We have therefore employed a further correction that we have already used for electron scattering from large polyatomic nonlinear targets with a good degree of success.[12,13] In particular, we will try to show how the combined effects of simplifying the exchange interaction between the bound electrons and the continuum projectile via a modified semiclassical (local) approach and of treating the correlation-polarization forces using a global functional model can indeed help us to deal with vibrationally inelastic collisions, at least for the present set of tetrahedral molecules, with a markedly reduced computational effort and with an acceptable reduction of accuracy.

C. Modeling the interaction

In order to include the long-range polarization term and the short-range dynamical correlation effects we have implemented a local, energy-independent model potential, $V_{\rm ecp}(\mathbf{r})$ for electron collisions which has already been discussed in our earlier work.[9–11] Briefly, the $V_{\rm ecp}$ model potential contains a short-range correlation contribution, $V_{\rm corr}$, which is smoothly connected to a long-range polarization contribution, $V_{\rm pol}$, both terms being specific for electron projectile. The short-range term is obtained by defining an average dynamical correlation energy of a single electron within the formalism of the Kohn and Sham variational orbitals representing the bound electrons. The functional derivative of such a quantity with respect to the SCF N-electron density of the molecular target provides a density functional description of the required short-range correlation term (for a general description of density functional theory methods see Parr and Yang[14]). The long-range part of $V_{\rm ecp}$ is obtained by first constructing a model polarization potential, $V_{\rm pol}$, which asymptotically agrees with the potential obtained from the static dipole polarizability of the target in its ground electronic state. This corresponds to including the dipole term in the second-order perturbation expansion of the polarization potential.

The new, full interaction now corresponds to carrying out the scattering equations using the static-exchange-correlation-polarization (SECP) description of the electron–molecule interaction.

In the present treatment of electron scattering from a nonlinear, polyatomic molecule we further employed a simpler form of exchange interaction in order to further reduce the computational complexity. Thus, we replaced the nonlocal contributions in Eq. (3) with a semiclassical approximate model, already employed and discussed by us in our earlier work (see, e.g., Refs. 15–17), which we called the semiclassical exchange (SMCE). It treats the bound-continuum exchange interaction more realistically than other simplified schemes (see, e.g., Ref. 18) in the sense that the local momentum of the bound electrons is initially disregarded with respect to that of the impinging particle thereby leading to the neglect of the gradients of molecular orbitals with respect to the gradient of the wave function for the projectile.[15–17]

Hence, the final expression of the exchange forces, $V_{\rm ex}^{\rm SMCE}(\mathbf{r}|k^2)$ is given by an energy-dependent function of the static interaction, $V_{\rm st}$, and the target total electron density in terms of its molecular orbitals (MOs), $\varphi_s(\mathbf{r})$,

$$V_{\rm ex}^{\rm SMCE}(\mathbf{r}|k^2)=\tfrac{1}{2}\{E-V_{\rm st}(\mathbf{r})\} - \frac{1}{2}\left\{[E-V_{\rm st}(\mathbf{r})]^2+8\pi\sum_{s=1}^{N}|\varphi_s(\mathbf{r})|^2\right\}^{1/2}, \tag{7}$$

where E is the asymptotic collision energy $E=\frac{1}{2}k^2$ and the index s runs over the occupied MOs of the target. $V_{\rm st}$ is the static interaction with the target electronuclear structure.

The coupled equation (3) can now be recast in an integral form by using[19,20] the potential coupling elements defined before, $V_{in}^{p\mu}(r|\mathbf{R})$, and employing standard Green's function techniques to obtain for the radial functions of the continuum electron

$$f_{ij}^{p\mu}(r|\mathbf{R}) = \delta_{ij}j_{li}(kr)+\sum_n \int_0^r dr'\; g_{li}(r,r')V_{in}(r'|\mathbf{R})f_{ij}^{p\mu}(r'|\mathbf{R}), \tag{8}$$

where the integral on the right-hand side of Eq. (8) terminates at $r'=r$ (integral equations with this property are called Volterra equations).

The numerical implementation and stabilization corrections for the equations given by Eq. (8) have been discussed for diatomics before[21–23] and we have recently[19,20] carried out its obvious generalization for polyatomic systems. Suffice it to say here that the combined use of a local form of exchange interaction (like the SMCE outlined before) with the integral formulation for the continuum solutions allows us to obtain the required K-matrix elements for each selected nuclear geometry with a substantial reduction of the computational time, a key element when dealing with vibrationally inelastic scattering calculations, even for very large partial wave expansions for Eq. (1).

III. THE VIBRATIONAL EXCITATION DYNAMICS

The crucial question when formulating a theoretical approach to the study of low-energy inelastic vibrational excitation of polyatomic molecules by electron impact is how to correctly include the effect of nuclear kinetic energy operators on the continuum wave functions for the scattered electron. From the earlier studies which went beyond some sort of weak-scattering approximations (clearly reviewed in Ref. 24) two types of approaches have been favored for diatomic targets: (i) one possibility rigorously takes into account the effects of the vibrational Hamiltonian by expanding the $(N+1)$ electron$+M$-nuclei system in a complete set of eigenfunctions of that Hamiltonian[25–27] thereby carrying out the vibrational close-coupling calculations, and (ii) another option is to approximate the above-mentioned effects by treating the internuclear coordinates as a set of parameters on which the scattering attributes will finally depend.[28–30] This approach constitutes the foundation of the adiabatic nuclear vibration (ANV) approximation and effectively extends the conventional Born–Oppenheimer (BO) theory of bound molecular states within a given electronic state to the continuum states of the whole electron–molecule system.

The latter formulation is computationally less demanding than the former but, at least in the case of diatomic targets,[31] and from our previous experience on a polyatomic molecule,[32] is known to introduce significant errors into the vibrationally inelastic cross sections for scattering energies near and within a few eV above the relevant excitation threshold, while turning out to be more realistic at higher collision energies.[32] As a result, very little experience has been gathered thus far on polyatomic targets' vibrational excitations by collision with electrons.

If one therefore starts by first making the observation that, at the collision energies of interest in most studies, the

molecular rotations can be considered as slower than the speed of the impinging electron, the rotational degrees of freedom can be eliminated from the scattering problem, which can then be formulated within a body-fixed (BF) frame of reference. In such an approximation, called the fixed-nuclear-orientation (FNO) scheme,[24,28] the reduced system wave function depends on two sets of coordinates only: the internal nuclear coordinates and the three coordinates of the continuum electron, **r** (mentioned earlier), $\Psi(\mathbf{r},\mathbf{R},\nu_0|E)$. The quantum number ν_0 collectively signifies the initial vibrational population which gives the molecular vibrational energy content by energy conservation as

$$E=\tfrac{1}{2}k_{\nu_0}^2+E_0=\tfrac{1}{2}k_\nu^2+E_\nu. \tag{9}$$

Here $k_{\nu_0}^2/2$ and $k_\nu^2/2$ are the projectile kinetic energies in the entrance and exit channels. If the zero energy is selected to be the vibrational ground state of the molecule, then the energy lost by an electron during the excitation process, $\Delta\epsilon_\nu$, is equal to E_ν.

If one now imposes further the continuum BO approximation on $\Psi(\mathbf{r},\mathbf{R},\nu_0|E_0)$, then one obtains the ANV approximation and the corresponding asymptotic behavior of the solutions is obtained by choosing the BF energy to be the incident kinetic energy of the projectile: $\frac{1}{2}k_0^2=E_0$. One then applies the (real) *K*-matrix boundary conditions for each set of $|\mathbf{R}|$ coordinates within each IR that contributes to the scattering[33–36]

$$u_{p\mu}^{ll_0}(r;\mathbf{R}_i)_{r\tilde{\to}\infty}\hat{j}_l(k_0r)\,\delta_{ll_0}+K_{ll_0}^{p\mu}(\mathbf{R})\hat{n}_l(k_0r), \tag{10}$$

where $\hat{j}$ and $\hat{n}$ are Riccati–Bessel and Riccati–Neuman functions.[37] The *T* matrix can then be obtained from the above-mentioned *K* matrix by writing (we disregard the explicit indication of the **R** dependence to simplify notation)

$$\underline{\mathbf{T}}=\underline{\mathbf{K}}(\underline{\mathbf{1}}-i\underline{\mathbf{K}})^{-1}. \tag{11}$$

The approximate FNO–ANV transition matrices can then be obtained by numerical quadratures over the relevant nuclear coordinates

$$T_{\nu_0 l_0,\nu l}^{p\nu}=\langle\chi|T_{l_0,l}(\mathbf{R})|\chi_{\nu_0}\rangle_{\mathbf{R}}, \tag{12}$$

where the χ's are the vibrational wave functions for the vibrational mode under consideration.

In the present exploratory study we will limit our analysis to the treatment of the totally symmetric breathing modes of some tetrahedral molecular targets.

IV. COMPUTED INTEGRAL CROSS SECTIONS

A. The elastic scattering results

As we discussed in the previous sections, the implementation of our model treatment of the electron–molecule interaction within the quantum coupled equations which describe the electron scattering process strongly reduces the computational effort but should be tested for its reliability in describing the relevant physics. In the following we will therefore show that the SCME potential and the CP potential models are able to reproduce reasonably well the elastic (rotationally summed) integral cross sections from the low energy regions of the Ramsauer–Townsend (RT) minima to the broad resonance features at higher energies.

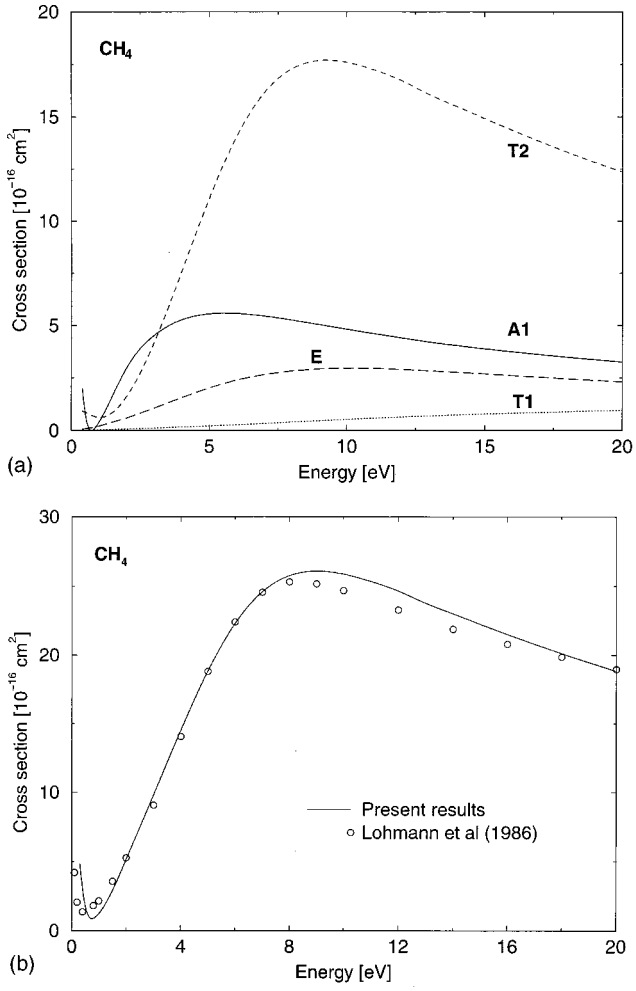

FIG. 1. Computed integral elastic cross sections (rotationally summed) using the SECP interaction modeling described in the main text. Top panel: Partial contributions from four different irreducible representations for the CH_4 target. Lower panel: Total computed values and experiments from Ref. 39.

In Fig. 1 we show, as an example, the computational results for the CH_4 molecule compared with experiments. The target electronic wave function was described by a SD, near-HF expansion which employed 1.082 Å as the equilibrium bond distance and the D95* basis set expansion. We used a dipole polarizability value of 17.5 a_0^3. The total electronic energy was found to be of -40.201 hartrees. The partial wave expansion of the potential was carried out up to $\lambda_{\max}=36$ and the continuum electron partial waves went up to $\lambda_{\max}=36$. These expansion values led to 20 coupled equations in the A_1 IR, 50 equations in T_2, and 30 in the E IR, respectively.

The top panel in Fig. 1 shows the energy dependence of the various IRs which contribute to the total elastic cross sections and they all exhibit the expected behavior, as was already found in earlier calculations on methane using the exact exchange interaction:[38] (i) the broad resonance feature before about 10 eV is mainly due to the t_2 symmetry of the continuum electron; (ii) the totally symmetric a_1 component

is responsible for the low energy RT minimum feature; and (iii) both the e and t_1 partial symmetries contribute the least to the size of the total elastic cross sections.

The bottom panel in Fig. 1 shows a direct comparison, on the same absolute scale, between our computed total elastic cross sections and the experimental values for the same observable.[39] One clearly sees that the present calculations follow very closely the experimental points and that the elastic cross sections are reproduced well by the model interactions we employ in this study. The computational effort for solving the coupled equations at one energy for *all* the contributing irreps was only of 200 s on a medium-size workstation.

Similar calculations were also carried out for the silane and the germane molecules to further test the reliability of our modelistic approach.

The basis set expansion for the target molecular orbitals (MOs) was at the D95* level, with a Si–H bond distance of 1.478 a_0 and a total electronic energy of -291.225 hartrees. The potential multipolar expansion went up to $\lambda_{max}=40$, which led to 24 coupled equations for the a_1, 60 for the t_2, and 37 for the l components, respectively. The α_0 value employed was 30.4 a_0^3.

For the GeH_4 molecule we employed a 6-311G $(6d,10f)$ basis set expansion, with a Ge–H bond distance of 1.523 Å and a total electronic energy of -2007.606 hartrees. The potential expansion went up to $\lambda_{max}=50$, which led to 35 coupled equations for the A_1, 56 for the E, and 91 for the T_2 irreps. The α_0 value employed was 34.4 a_0^3.

The results of the present calculations, in the same fashion as those shown in Fig. 1, are now given in Fig. 2 for the silane target and in Fig. 3 for the germane case.

We see in Figs. 2 and 3 that the agreement for the SiH_4 calculation is nearly as good as that found for CH_4, while the computed results for GeH_4 turn out to have the same shape as the experiments but yield integral cross sections which are about 20% larger than the measurements, with the largest differences being below 4 eV of energy.[40]

The experimental data for the latter molecule are, however, much fewer and therefore, in contrast with the better known situations of CH_4 and SiH_4, the comparison with our calculations could not be carried out as extensively as in the other two examples. Specifically, our earlier calculations[45,46] on the elastic differential cross sections for GeH_4 used the model treatment of exchange forces and found very good agreement in the comparison between computed and measured angular distributions. Thus, we feel that the use of model exchange treatment for integral cross sections would require a more extensive comparison with other experiments before being declared not realistic for the germane system. On the whole, however, we see that our modeling of the interaction forces is providing here an acceptable description of the elastic scattering for the three molecules examined.

The computed cross sections for the elastic integral cross sections of all of them are reported, for completeness, in Table I at the collision energies of the present study. All results are considered to be converged within 5%. Each energy calculation required around 100 s on a Digital workstation with a single processor, thus underlining once more the appealing computational simplicity of the present SMCE-CP modeling of the interaction forces.

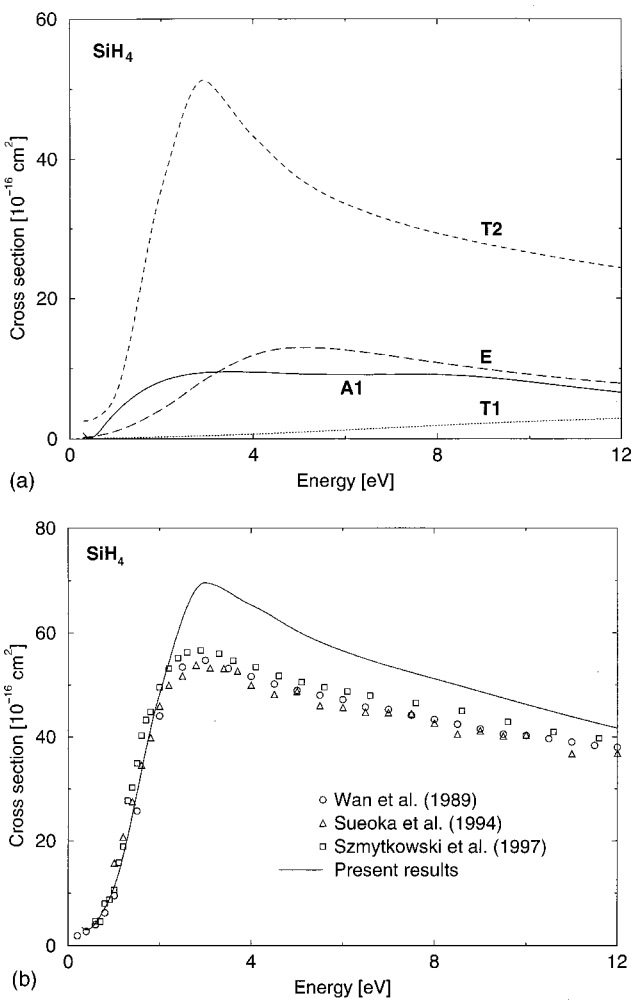

FIG. 2. Same as in Fig. 1 but for the silane molecular targets. The experimental data are from Refs. 41–43.

Because of this marked reduction of the computational effort when using the present model of exchange–correlation forces, it seems reasonable to now extend it to the treatment of vibrationally inelastic processes.

B. The vibrationally inelastic cross sections

As discussed in the earlier sections, the ANV approach to the evaluation of vibrational inelasticity by electron impact requires the solution of the scattering problem over a broad range of nuclear coordinates and the corresponding quadrature of the T-matrix values over the initial and final vibrational wave functions [see Eq. (12)]. In the present, exploratory calculations we have considered first the totally symmetric breathing modes of each tetrahedral molecule, since this vibration usually requires a large amount of energy transfer by electron impact. We have already seen for the case of the CH_4 target[32] that the four normal-mode excitation cross sections are comparable with each other in size and that our earlier computed values compared well with experimental findings.[39] Furthermore, our more recent study on the ANV approach for all four normal modes of CH_4 (Ref. 47)

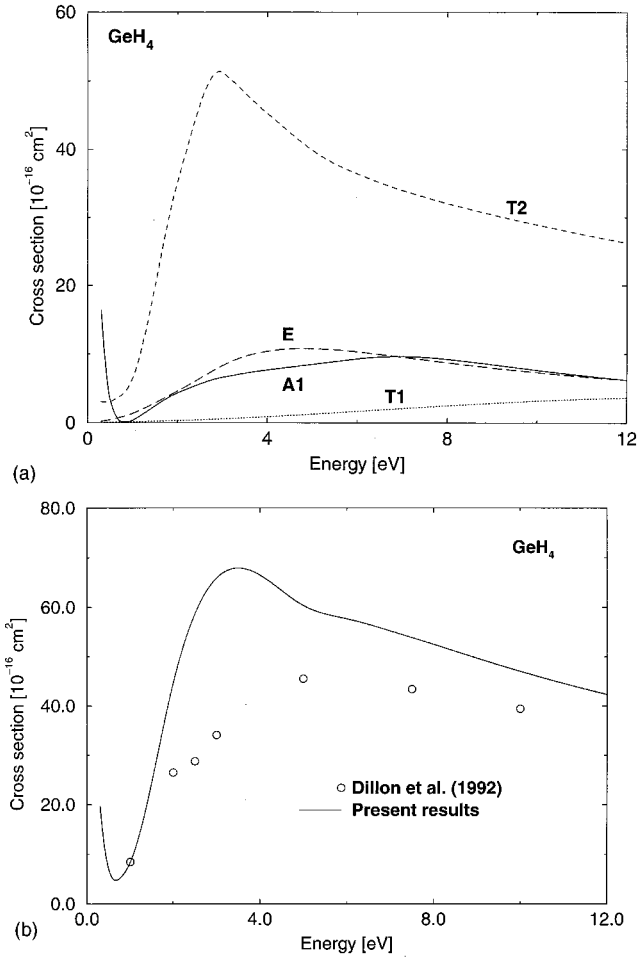

FIG. 3. Same as in Figs. 1 and 2 but now for the germane molecule. The experiments are from Ref. 44.

employed both the exact exchange and the present SMCE model and found between them differences in size of no more than 20% and an improved accord with the existing experiments. Thus, to start with the ν_1-mode excitation could also provide realistic estimates of the total excitation cross sections for the other two tetrahedral molecules we are studying here. The calculations were carried out over a range of 15 values of the internuclear distances, going from $R_{\min}=0.9$ Å to $R_{\max}=1.35$ Å for CH_4, from 1.25 to 1.75 Å for SiH_4, and from 1.30 to 1.80 Å for GeH_4. The corresponding potential energy curves were interpolated numerically and employed to numerically generate the quantum vibrational wave functions for the first four vibrational levels of the three molecules. The energy separations between the bound states are shown in Table II. The numerical quadrature of Eq. (12) was carried out to convergence down to less than 1% variations. Figures 4 and 5 report our calculations for the $(0\rightarrow 1)$ inelastic cross sections compared for CH_4, SiH_4, and GeH_4 over the range of collision energy discussed before. The contributions from the various symmetry components are also shown for each target molecule. The following comments could be readily made.

TABLE I. Elastic scattering. Integral cross section (Å^2).

E (eV)	CH_4	SiH_4	GeH_4
1.00	1.231	11.166	8.330
2.00	−5.165	48.372	44.805
3.00	9.828	69.552	66.620
4.00	14.537	65.293	64.127
5.00	18.870	60.326	60.359
6.00	22.322	56.530	58.374
7.00	24.602	53.629	55.206
8.00	25.769	51.152	52.492
9.00	26.095	48.702	49.687
10.00	25.880	46.223	47.018
11.00	25.349	43.856	44.564
12.00	24.657	41.670	42.325

TABLE II. Computed energy spacings between the bound vibrational levels of the ν_1-mode vibrations for the target molecules. The harmonic oscillator values are shown at the bottom. (All values are in cm^{-1}).

	CH_4	SiH_4	GeH_4
$\Delta\epsilon_{01}$	3125.95	2314.88	2267.24
$\Delta\epsilon_{02}$	6230.61	4615.59	4519.32
$\Delta\epsilon_{03}$	9313.58	6902.54	6755.59
$\Delta\epsilon_{12}$	3104.66	2300.71	2252.08
$\Delta\epsilon_{\text{harmonic}}$	3147.39	2328.62	2283.20

(i) The resonance supported by the t_2 component contributes the most to the vibrationally inelastic process in all molecules, in agreement with the relevant physics of the excitation.

(ii) The totally symmetric a_1 component provides sizable contributions to the inelastic process beyond the main resonance region and, for silane and germane, suggests that a second, higher-energy resonant feature can exist in this inelastic channel.

(iii) As expected, the two other symmetry components to the continuum electron, e and t_1, yield negligible contributions to the excitation mode of the ν_1.

(iv) All ANV cross sections do not correctly vanish at threshold because of the energy mismatch inherent to the method. Hence, as already discussed before, we cannot use

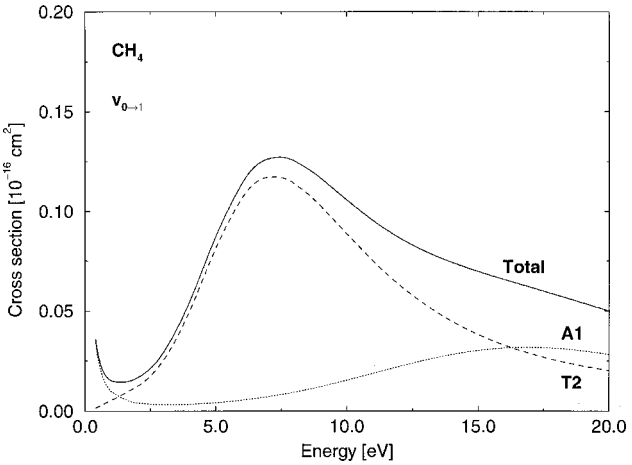

FIG. 4. Vibrationally inelastic cross sections for the $(0\rightarrow 1)$ excitation of the ν_1 mode of CH_4. The partial contributions from two IRs and the total cross section are shown.

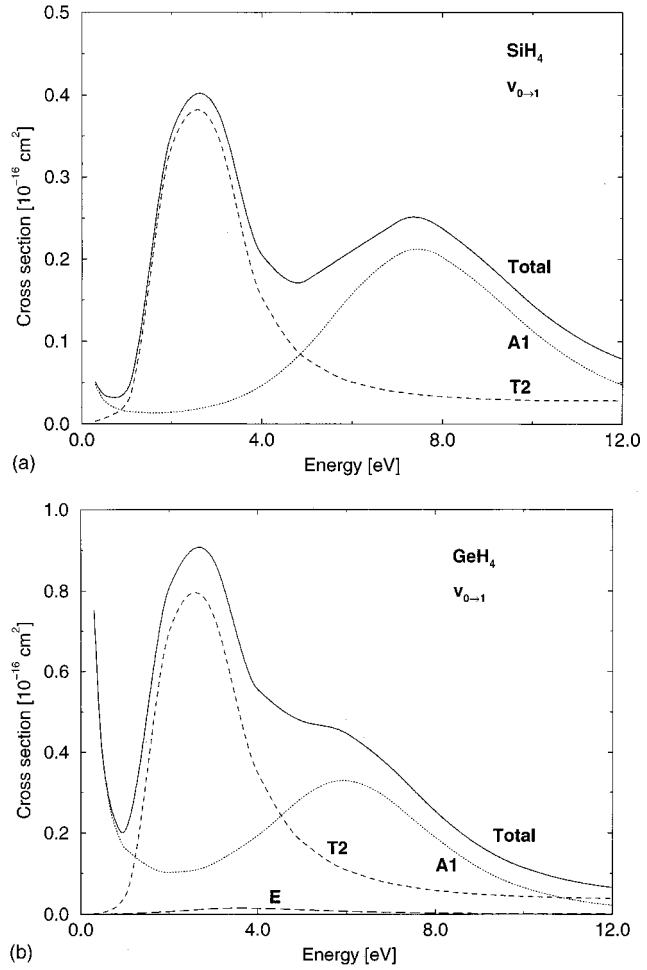

FIG. 5. Same as in Fig. 4 but for the SiH_4 molecule (top panel) and for the GeH_4 molecule (lower panel).

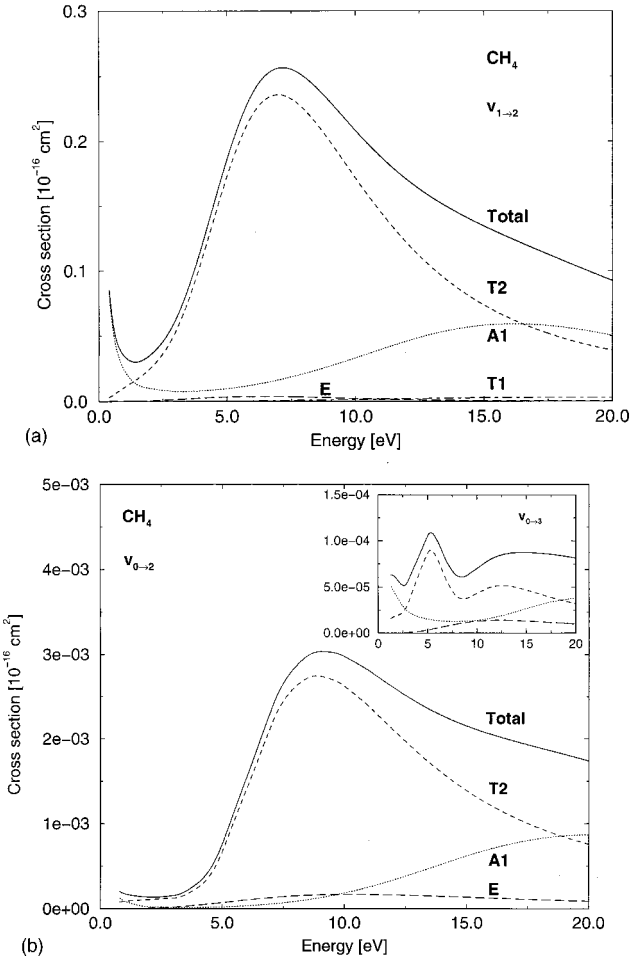

FIG. 6. ''Hot'' band excitation cross section (top panel) and multiple quantum excitations (lower panels) for the CH_4 molecule. The partial contributions shown refer to the t_2 IR (dashed lines), to the a_1 IR (dotted lines), and to the e IR (long dashes).

computed values below about 2.0 eV (see our earlier tests in Ref. 32).

(v) The scattering process yields fairly small cross sections for all systems, although it markedly increases when going from CH_4 ($\sim 0.15\times 10^{-16}$ cm^2) to SiH_4 ($\sim 0.40\times 10^{-16}$ cm^2) to GeH_4 ($\sim 0.9\times 10^{-16}$ cm^2) at the resonances.

Given the limited decrease of the energy spacings from methane to germane (see Table II), these results are in keeping with physical expectations and suggest that the electron collision excitation mechanisms require the coupling with the bound electrons as the chief driving force. Hence, the larger number of such electrons in going from CH_4 to GeH_4 causes stronger couplings and more efficient dynamical distortions of the target molecules.

In the excitation processes that play an important role when modeling molecular plasmas the presence of ''hot'' molecules and of multiple quantum excitations has been found to be significant in simpler diatomics like H_2, N_2, and O_2.[2,48] It therefore becomes of interest to see what would be the role of such inelastic processes in the present case. Figures 5–7 therefore report the behavior of the inelastic processes from $n=1$ (top panels) and that of the multiple quantum transitions (lower panels). In the insets of the lower panels the $\Delta n=3$ excitation cross sections are also shown. Here again the following comments could be made.

(i) The excitations of ''hot'' molecules turn out to occur with larger probabilities than the excitations of molecules in their $n=0$ initial vibrational state. We see, in fact, that the corresponding cross sections of methane, silane, and germane for the $(1\rightarrow 2)$ excitations are about 50% larger than their counterparts for the $(0\rightarrow 1)$ excitations. This result is in keeping with what was found to occur for H_2 and N_2 excitation by electron impact.[1–3]

(ii) The multiple excitation cross sections shown in the lower panels (and in the insets) of Figs. 5–7 clearly indicate that their corresponding probability is markedly reduced by one or more orders of magnitude: the weak coupling induced by the potential is not able to overcome the strong orthogonality between vibrational functions that therefore reduces the size of the integral in Eq. (14).

(iii) The additional a_1-type resonant enhancement, seen in the inelastic channels for the $\Delta n=1$ excitations from the $n=0$ initial states, persists in the case of excitation from vibrationally hot targets and becomes even more important for the multiple quantum excitations. We see, in fact, from the insets that the $\Delta n=3$ excitations show larger contribu-

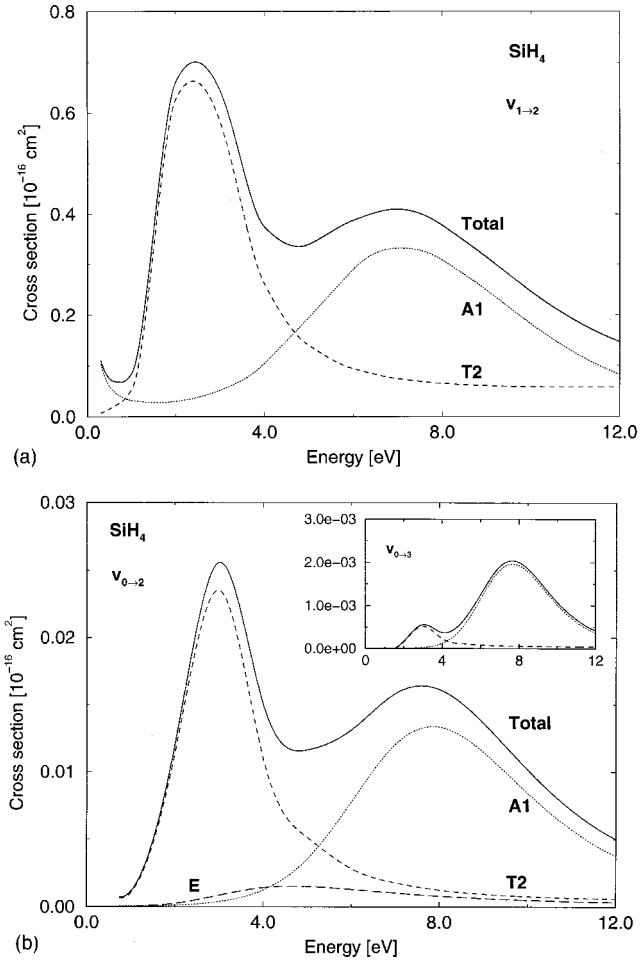

FIG. 7. Same as in Fig. 6 but for the target molecule SiH_4. All the symbols used have the same meaning as before.

tions from this higher-energy resonance than from the t_2 type of resonance.

To be more specific, we finally report in Tables III and IV all the present computed values for all the excitation cross sections considered.

In conclusion, we have seen for all three systems that the dominant contribution to the ν_1 excitation comes from single-quantum energy transfers and that an initially increased population of higher vibrational levels in the target molecule enhances the probability of transferring energy by electron impact. We will therefore analyze a bit more in detail in Sec. IV C the actual behavior of some indicators of collisional excitation efficiency that could be obtained from the computed state-to-state cross sections.

C. Excitation efficiency and excitation rates

One of the simplest quantities to evaluate from the inelastic cross sections is the average energy transfer, $\langle \Delta E \rangle_0$, from the initial vibrational level $n=0$, usually considered the dominantly populated level in the low-temperature molecular plasmas:

$$\langle \Delta E \rangle_0 = \frac{\Sigma_{n\neq 0}^{\infty}\ \sigma_{(0\to n)} \Delta \epsilon_i}{\Sigma_{n=0}^{\infty}\ \sigma_{(0\to n)}}, \tag{13}$$

TABLE III. CH_4, vibrational excitation (ν_1). Integral cross section (Å^2).

E (eV)	$\sigma_{0\to1}$	$\sigma_{0\to2}$	$\sigma_{0\to3}$	$\sigma_{1\to2}$
0.4	0.036	⋯	⋯	0.0855
0.6	0.023	⋯	⋯	0.0537
0.8	0.017	0.0002	⋯	0.0405
1.0	0.015	0.0002	⋯	0.0344
2.0	0.016	0.0001	5.7(−05)	0.0352
3.0	0.029	0.0001	5.6(−05)	0.0625
4.0	0.055	0.0003	8.0(−05)	0.1177
5.0	0.087	0.0008	1.05(−04)	0.1861
6.0	0.114	0.0015	1.0(−04)	0.2374
7.0	0.126	0.0023	7.6(−05)	0.2564
8.0	0.125	0.0029	6.2(−05)	0.2497
9.0	0.116	0.0030	6.3(−05)	0.2305
10.0	0.105	0.0030	7.0(−05)	0.2082
11.0	0.095	0.0028	7.8(−05)	0.1876
12.0	0.087	0.0026	8.3(−05)	0.1704
13.0	0.080	0.0024	8.6(−05)	0.1563
14.0	0.074	0.0023	8.7(−05)	0.1446
15.0	0.070	0.0021	8.7(−05)	0.1345
16.0	0.066	0.0020	8.7(−05)	0.1254
17.0	0.062	0.0020	8.6(−05)	0.1168
18.0	0.058	0.0019	8.5(−05)	0.1084
19.0	0.054	0.0018	8.3(−05)	0.1003
20.0	0.5	0.0017	8.1(−05)	0.0924

a quantity given in units of meV over the range of considered collision energies (Fig. 8).

The results are shown in the upper panel of Fig. 9 and we clearly see there the effects of the different resonant features exhibited by corresponding cross sections.

(i) In the energy range from 2.0 to about 6.0 eV the resonant cross sections of the germane system provide the largest energy transfer values since both CH_4 and SiH_4 become more efficient only at the higher collision energies.

(ii) The methane molecule shows the smallest efficiency in the low energy range since its resonant behavior begins to play a role only from 8 eV and beyond.

(iii) At the higher collision energies the energy examined, transfer values for the methane target are the largest for the three systems, with SiH_4 and GeH_4 becoming similar to each other (and much smaller than CH_4) beyond 8 eV.

The numerical values of the computed ΔE of Fig. 9 are reported in Table V.

Another quantity of interest in this context is the collisional heating function, CHF, which is defined as the ratio between a chosen inelastic process and the overall flux into the (elastic+inelastic) channels.[49] In the case of the vibrational excitation of the ν_1 mode only, its definition becomes

$$\mathrm{CHF}(T,n) = \int \mathrm{CHF}(E,n) f(E,T) dE \tag{14}$$

and

$$\mathrm{CHF}(E,n) = \frac{\Sigma_{n\neq 0}^{\infty}\ \sigma_{(0\to n|E)}}{\Sigma_{n=0}^{\infty}\ \sigma_{(0\to n|E)}}, \tag{15}$$

where $f(E,T)$ is a Boltzmann energy distribution function for the beam of impinging electrons and a given number density, d, of the molecule in units of mol cm^{-3}.

TABLE IV. (a) SiH_4, vibrational excitation (ν_1). Integral cross section (Å^2). (b) GeH_4, vibrational excitation (ν_1). Integral cross section (Å^2).

	E (eV)	$\sigma_{0\to1}$	$\sigma_{0\to2}$	$\sigma_{0\to3}$	$\sigma_{1\to2}$
(a)	0.30	0.0508	⋯	⋯	0.109
	0.50	0.035	⋯	⋯	0.074
	0.75	0.031	0.0007	⋯	0.067
	1.00	0.402	0.0011	0.0003	0.084
	2.00	0.3544	0.0117	0.0002	0.660
	3.00	0.3816	0.0247	0.0006	0.644
	4.00	0.2047	0.0136	0.0004	0.374
	5.00	0.1744	0.0101	0.0006	0.339
	6.00	0.2102	0.0118	0.0013	0.387
	7.00	0.2454	0.0148	0.0019	0.409
	8.00	0.2370	0.0154	0.0020	0.377
	9.00	0.1934	0.0130	0.0016	0.314
	10.00	0.1441	0.0097	0.0010	0.245
	11.00	0.1050	0.0068	0.0006	0.188
	12.00	0.0785	0.0047	0.0004	0.146
(b)	0.30	0.751	⋯	⋯	1.746
	0.50	0.378	⋯	⋯	0.883
	0.75	0.238	0.0111	⋯	0.556
	1.00	0.205	0.0082	0.0006	0.474
	2.00	0.809	0.0255	0.0037	1.665
	3.00	0.875	0.0228	0.0028	1.631
	4.00	0.555	0.0163	0.0023	1.056
	5.00	0.476	0.0216	0.0041	0.846
	6.00	0.445	0.0252	0.0051	0.746
	7.00	0.360	0.0215	0.0039	0.563
	8.00	0.252	0.0143	0.0021	0.414
	9.00	0.167	0.0085	0.0010	0.293
	10.00	0.114	0.0052	0.0005	0.202
	11.00	0.083	0.0030	0.0003	0.155
	12.00	0.065	0.0020	0.0002	0.127

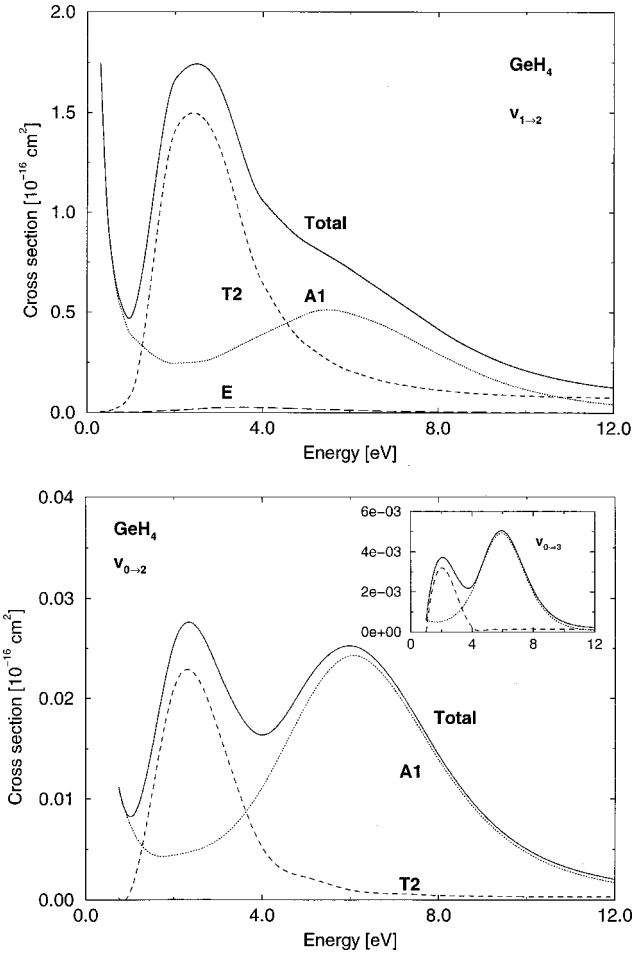

FIG. 8. Same as in Figs. 6 and 7 but for the target molecule GeH_4. See their captions for the meaning of symbols.

The temperature dependence of such quantities for the ν_1 mode of each molecule is shown in the lower two panels of Fig. 9, where on the left-hand side we report the range of values from 1000 to 4000 K and on the right-hand side the values from 4000 to 10 000 K. In all cases we consider excitation from the $n=0$ level only. The germane gas clearly shows the largest excitation function which becomes even more so in the higher interval of temperature. All values are, however, fairly small and become significant for an electron ''heating'' of the ambient gas only above about 5000 K. As expected, the CH_4 molecule exhibits the smallest efficiency, due both to its vibrational force constant being the largest of them all (see Table II) and to its smaller dipole polarizability.

One should keep in mind, however, that the energies of the electrons at the above-mentioned temperatures are below the region where the ANV is expected to be valid and therefore it is difficult to assess here the level of reliability for such quantities. It is, on the other hand, still useful to analyze each behavior relative to the other for the three systems.

The next global quantities of interest are the individual, state-to-state, excitation rates, this time as a function of the ambient gas temperature

$$K_{n\to n'}(T)=4\pi\left(\frac{1}{2\pi k_B T}\right)^{3/2} \times d\int_0^\infty \sigma_{n\to n'}\exp\left(-\frac{v^2}{2k_B T}\right)v^3 dv, \qquad (16)$$

where k_B is the Boltzmann constant and v the electron relative velocity in the gas. Here d is the molecular number density.

The computed values for the three systems studied here are presented in Figs. 10(a), 10(b), and 10(c) for the excitation rates from the $n=0$ level, the most probable of the molecular states being populated at the temperatures of interest. We should also note here again that, although the range of T being shown is that of interest in the plasma deposition processes,[2] the corresponding electron impact energies are still below the expected range of full validity of the ANV reduction. Hence, the absolute level of reliability of these results is hard to evaluate.

(i) All rates, as expected, are remarkably small and invariably show the ones associated with the $\Delta n=1$ excitations to be the largest.

(ii) The size of the rates clearly increases from methane [Fig. 10(a)] to germane [Fig. 10(c)] although they all tend to essentially the same high-T limiting values of $\sim 10^{-37}$ cm^3 s^{-1}.

(iii) All the multiple excitation processes are much smaller and remain so even at their highest ''saturation'' temperatures shown. There one sees that the $\Delta n=2$ excitations are more than one order of magnitude smaller than

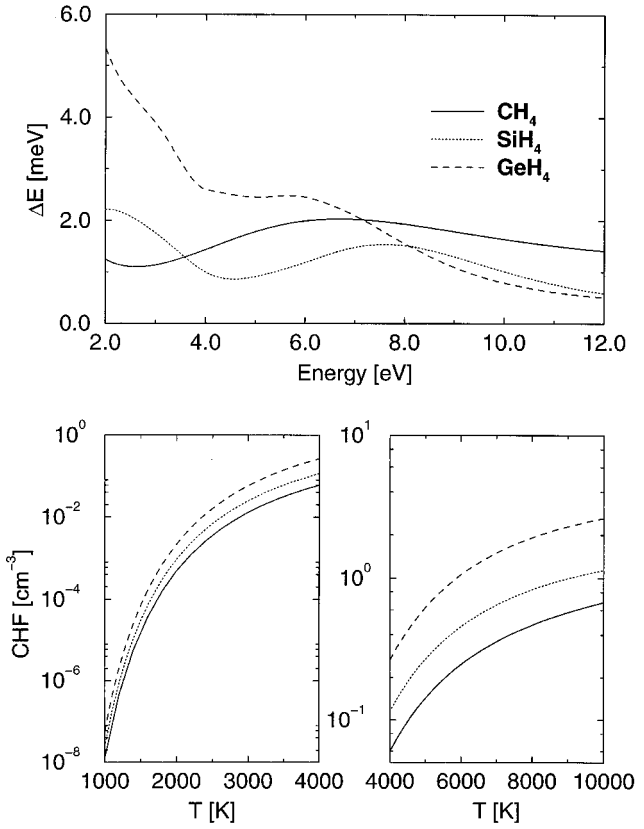

FIG. 9. Computed average energy transfers (upper panel) as a function of collision energy for the three molecules discussed in this work. The lower panels show, over two different ranges of temperature, the behavior of the computed collisional heating efficiency, CHF, defined in the main text.

$\Delta n=1$ and the $\Delta n=3$ excitations are about three orders of magnitude smaller.

V. PRESENT CONCLUSIONS

In the present work we have explored the computational feasibility of modeling via nonempirical approximations the vibrational excitation cross sections by collision with electrons of three tetrahedral molecules.

In particular, we have tried to show that the combined use of simplified interaction potentials and adiabatic dynamics is capable of providing a rather realistic description of electron scattering total elastic cross sections (integral) at low collision energies with considerable savings of computational time. For the excitation processes, however, the only possible comparison, given the scant experimental data, has been for the case of CH_4, where the ANV and the off-shell results already reported in our earlier work[32] were compared with the same experiments.[47] The more approximate ANV dynamical coupling was found to be rather realistic, when compared with off-shell results, above about 2 eV of electron

TABLE V. Computed average energy transfer values (meV).

E (eV)	CH_4	SiH_4	GeH_4
2.0	1.261	2.299	5.366
3.0	1.171	1.775	3.871
4.0	1.475	1.021	2.584
5.0	1.820	0.932	2.458
6.0	2.029	1.202	2.441
7.0	2.057	1.495	2.098
8.0	1.962	1.528	1.480
9.0	1.815	1.316	1.059
10.0	1.666	1.032	0.752
11.0	1.539	0.788	0.568
12.0	1.442	0.613	0.466

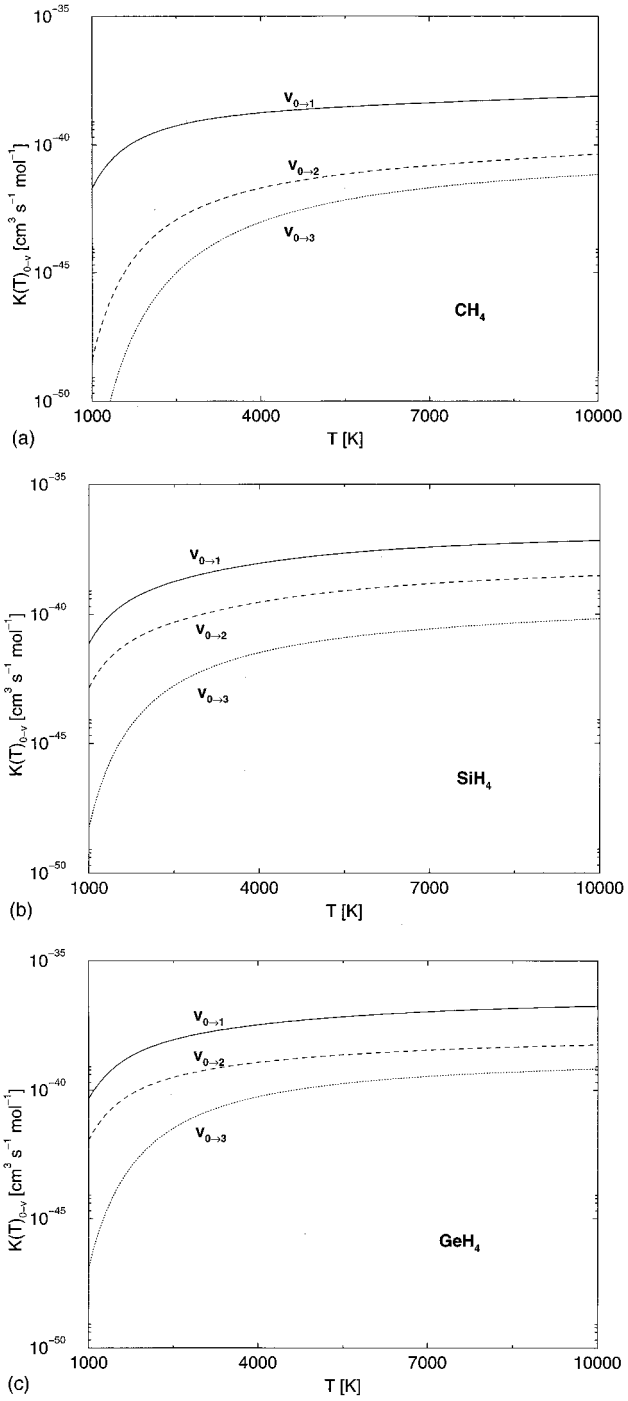

FIG. 10. Computed state-to-state excitation rates for the CH_4, SiH_4, and GeH_4 molecules as a function of temperature. The rates shown in (a) correspond to $\Delta n=1$, 2, and 3 excitations from the $n=0$ initial level of the ν_1 mode of methane. The results shown in (b) refer to the calculations for the SiH_4 molecule. (c) The same calculations for the GeH_4 molecule.

collision energy. We have also found that exact exchange and SMCE exchange yielded cross sections for all four modes at most about 20% smaller for the latter than for the former. Because of the large errors on the experimental data, however, both calculations fitted well the existing data.[47]

The present study, albeit still preliminary, allows us to make the following comments.

(i) The use of the SMCE exchange interaction and of the V_{cp} modeling of the correlation-polarization forces has shown that one can obtain, at least for CH_4 and SiH_4, a realistic description of the elastic scattering process and rather good accord with the experimentally measured integral cross sections. Furthermore, the earlier calculations[46] of the germane elastic angular distributions with model exchange turned out to be very close to experiments and provided integral cross sections very similar to the ones from the present calculations with the SMCE model exchange.

(ii) The ANV calculations for CH_4 had been shown by us[32,39] to be in good agreement with the more accurate off-shell method once one is away from the $(0\rightarrow1)$ excitation threshold. Hence, the CH_4 results with exact exchange[47] gave us some level of confidence on the reliability of approximate exchange models, at least for hydrates. It also encouraged us to use their extension to other polyatomic targets with a better confidence on their reliability, in spite of its being not yet directly tested with experiments because of the lack of them.

(iii) The computed cross sections are all fairly small in size, with more marked contributions appearing in the energy range of the shape resonances of t_2 symmetry which exist, for all three molecules, in both the elastic and the inelastic channels. The heavier systems like SiH_4 and GeH_4 show in the ν_1-mode inelastic channels (at higher collision energies) the additional presence of a broad resonance of a_1 symmetry.

(iv) The heating efficiency and the energy loss efficiencies, at the temperatures of interest in molecular plasmas, turn out to be fairly small for the ν_1 vibrational mode and for all three molecules. The present calculations also indicate that the excitation efficiency is larger for silane and germane, the latter molecule being the most efficient energy ''sink'' for the electrons in the beam, as seen from the state-to-state excitation rates of Figs. 10(a), 10(b), and 10(c).

The general features shown by the excitation of the ν_1 mode in the three target molecules are not expected to be very different when the other modes will be considered, as we have recently found for CH_4.[47] From those findings,[47] in fact, we can qualitatively predict that the total energy-loss values coming from the global excitations of the four modes of the tetrahedral targets should yield $\langle \Delta E \rangle$ estimates for each molecule which are about six to eight times larger than those coming only from the ν_1 excitation.

In conclusion, we think that the present data are already telling us that our proposed modeling of the e^-–molecule interaction and of the ANV vibrationally inelastic dynamics markedly reduces the computational requirements and makes it possible for us to obtain the range of microscopic data needed to explore the physics of electron-impact vibrational excitations in polyatomic molecular gases. Although its level of reliability has only been checked on the methane target and on the elastic collision processes of all three molecules, we would still be able to employ this modeling for a more detailed analysis of the interplay between structural properties of a given molecular target gas and the dynamics of its interaction with electron beams of energy well above the vibrational thresholds, thereby providing further possible comparisons with experiments on other systems.

ACKNOWLEDGMENTS

The financial support from The Italian National Research Council (CNR) and The Italian Ministry for University and Research (MURST) is here acknowledged. We also thank The Research Grant Committee of the University of Rome and the Max-Planck Research Award for further financial support. One of us (R.C.) thanks the CASPUR Consortium for a study grant that supported his stay in Rome during the completion of this work.

[1] L. G. Christophorou, D. L. McCorckle, and A. A. Christodoulides, in *Electron–Molecule Interactions and Their Applications*, edited by L. G. Christophorou (Academic, New York, 1984), p. 477.
[2] M. Capitelli, R. Celiberto, and M. Cacciatore, Adv. At., Mol., Opt. Phys. **33**, 321 (1994).
[3] R. Celiberto and T. Rescigno, Phys. Rev. A **47**, 1939 (1993).
[4] A. V. Phelps and L. C. Pitchford, JILA Inf. Center Report No. 26 (1985).
[5] W. H. Huo and H. T. Trummel, in *Molecular Physics and Hypersonic Flow*, edited by M. Capitelli (Kluwer, Dordrecht, 1996).
[6] Y. Itikawa, Int. Rev. Phys. Chem. **16**, 155 (1996).
[7] *Computational Methods for Electron–Molecule Collisions*, edited by W. H. Huo and F. A. Gianturco (Plenum, New York, 1995).
[8] F. A. Gianturco and A. Jain, Phys. Rep. **143**, 347 (1986).
[9] A. Jain and F. A. Gianturco, J. Phys. B **24**, 2387 (1991).
[10] F. A. Gianturco and R. Lucchese, J. Phys. B **29**, 3955 (1996).
[11] F. A. Gianturco, R. Lucchese, and N. Sanna, J. Chem. Phys. **104**, 6482 (1996).
[12] F. A. Gianturco and R. Lucchese, J. Chem. Phys. **108**, 6144 (1998).
[13] F. A. Gianturco and R. Lucchese, Chem. Phys. Lett. **301**, 456 (1999).
[14] R. G. Parr and W. Yang, *Density Interactions Functional Theory of Atoms and Molecules* (Oxford University Press, Oxford, 1989).
[15] M. E. Riley and D. G. Truhlar, J. Chem. Phys. **63**, 2182 (1975).
[16] F. A. Gianturco and S. Scialla, J. Chem. Phys. **87**, 6468 (1987).
[17] F. A. Gianturco and S. Scialla, Phys. Rev. A **36**, 557 (1987).
[18] S. Hara, J. Phys. Soc. Jpn. **22**, 710 (1967).
[19] R. Curik, F. A. Gianturco, and N. Sanna, J. Phys. B **33**, 615 (2000).
[20] R. Curik, F. A. Gianturco, and N. Sanna, Int. J. Quantum Chem. (submitted).
[21] T. N. Rescigno and A. E. Orel, Phys. Rev. A **24**, 1267 (1981).
[22] T. N. Rescigno and A. E. Orel, Phys. Rev. A **25**, 2402 (1982).
[23] W. N. Sams and D. J. Kouri, J. Chem. Phys. **51**, 4809 (1969).
[24] N. F. Lane, Rev. Mod. Phys. **52**, 29 (1980).
[25] N. Chandra and A. Temkin, Phys. Rev. A **13**, 188 (1976).
[26] M. A. Morrison and W. K. Trail, Phys. Rev. A **48**, 2874 (1993).
[27] M. A. Morrison and W. Sun, in *Computational Methods for Electron–Molecule Collisions*, edited by W. Huo and F. A. Gianturco (Plenum, New York, 1995), p. 131.
[28] D. M. Chase, Phys. Rev. **104**, 838 (1956).
[29] M. Shugard and A. U. Hazi, Phys. Rev. A **12**, 1895 (1975).
[30] F. H. M. Faisal and A. Temkin, Phys. Rev. Lett. **28**, 203 (1972).
[31] A. N. Feldt, M. A. Morrison, and B. C. Saha, Phys. Rev. A **30**, 2811 (1984).
[32] S. C. Althorpe, F. A. Gianturco, and N. Sanna, J. Phys. B **28**, 4165 (1995).
[33] M. A. Morrison, M. Abdolsalami, and B. K. Elza, Phys. Rev. A **43**, 3440 (1991).
[34] T. N. Rescigno, C. W. McCurdy, A. E. Orel, and B. H. Lengsfield III, in *Electron Collisions with Molecules, Clusters and Surfaces*, edited by H. Ehrhardt and L. A. Morgan (Plenum, New York, 1994), p. 1.
[35] H. T. Thümmel, R. K. Nesbet, and S. D. Peyerimhoff, J. Phys. B **25**, 4533 (1992).
[36] S. Mazevet, M. A. Morrison, O. Boydstun, and R. K. Nesbet, J. Phys. B **32**, 1269 (1999).

[37] See, e.g., J. R. Taylor, *Scattering Theory* (Wiley, New York, 1972).
[38] F. A. Gianturco, J. A. Rodriguez-Ruiz, and N. Sanna, Phys. Rev. A **52**, 1257 (1995).
[39] See references quoted in F. A. Gianturco, N. Sanna, C. T. Bundschu, J. C. Gibson, R. J. Culley, M. J. Brunger, and S. J. Buckman, J. Phys. B **30**, 2239 (1997).
[40] F. A. Gianturco, R. R. Lucchese, N. Sanna, and A. Talamo, in *Electron Collisions with Molecules, Clusters, and Surfaces*, edited by H. Ehrhardt and L. A. Morgan (Plenum, New York, 1994), p. 71.
[41] H. X. Wan, J. H. Moore, and R. Tossell, J. Chem. Phys. **92**, 7340 (1989).
[42] O. Sueoka, S. Mori, and A. Hameda, J. Phys. B **27**, 1453 (1994).
[43] Cz. Szmytkowski, P. Mozijko, and G. Kasperki, J. Phys. B **30**, 1863 (1997).
[44] M. A. Dillon, L. Boester, H. Tanaka, M. Kimura, and H. Saro, J. Phys. B **26**, 3147 (1993).
[45] K. L. Baluya, A. Jain, V. Di Martino, and F. A. Gianturco, Europhys. Lett. **17**, 139 (1992).
[46] A. Jain, K. L. Baluya, V. DiMartino, and F. A. Gianturco, Chem. Phys. Lett. **183**, 34 (1992).
[47] M. Cascella, R. Curik, F. A. Gianturco, and N. Sanna, J. Phys. B (to be published).
[48] *Novel Aspects of Electron–Molecule Collisions*, edited by K. H. Becker (World Scientific, Singapore, 1998).
[49] E. Bodo, S. Kumar, F. A. Gianturco, M. Raimondi, and M. Sironi, J. Phys. Chem. A **102**, 9390 (1998).